Switching in $KNbO_3$ single crystals containing cooperatively ordered impurity dipoles

S. G. Ingle and J. G. Dupare
Laxminarayan Institute of Technology, Nagpur University, Nagpur, India
(Received 26 February 1991)

In $KNbO_3$ single crystals having an impurity dipole content of about 10^{16} m^{-3} it is found that switching is strongly affected by the presence of these dipoles, and the hysteresis loop shape can be correlated to the domain structure that itself is determined by the distribution of the impurity dipoles that have cooperative ordering among them. A theoretical model for the shape of the loop has been developed considering nucleation of microdomains by the impurity dipoles and their subsequent evaporation under the reversed electric field. The model is found to describe well the observed hysteresis loops traced at various frequencies. The effect of clamping produced by external compressive forces or dc bias fields can also be understood in terms of the ideas used in the development of the model. The measurements carried out at various temperatures show that the effect of the dipoles in the loops is shown more prominently with higher temperatures. The nature of the switching transients using square-wave pulses confirms that the nucleation and growth mechanism suggested by Merz is only partially operative, as the process becomes strongly dependent on the role of the impurity dipoles.

I. INTRODUCTION

The hysteresis loop represents a characteristic ferroelectric behavior, the actual shape of the loop depending upon the domain structure. The response of the domain structure involves nucleation and growth of domains,[1] and any mechanism that significantly affects either of these processes must also affect the hysteresis loop shape correspondingly. The recent studies by Ingle and co-workers[2–9] on nucleation of microdomains by the impurity dipoles in $KNb0_3$ single crystals showed that, for crystals containing density of impurity dipoles of the order of 10^{16} m^{-3}, the effect of the dipoles on domain formation is so strong that, at times, the entire domain structure is formed by these dipoles. It was therefore felt necessary to see how this process is reflected in the hysteresis loop shapes.

Fousek and Berezina[10] reported as early as 1964 that the hysteresis loops get distorted at high frequencies owing to the change in the response of the domains to the applied varying electric field. Since then, many workers have reported significant changes in the loops, and most of them attributed these changes to defects in crystals. The generation of internal bias fields,[11–14] stabilization of domain structure by dislocations,[15] vacancies,[16] elastic dipoles,[17,18] and impurity ions[19] are usually the mechanisms suggested. However, the peculiar behavior observed in the present studies could not be satisfactorily explained in terms of any of these mechanisms. A theoretical model to be presented in this paper based on nucleation of microdomains and their evaporation under the reversed field was therefore developed, and it is found that the observation of the hysteresis loop shapes under a variety of conditions of tracing frequency, temperature, and external clamping by mechanical or electrical means can be readily understood in terms of this model. A general background necessary to appreciate the model is presented first in the next section.

II. PERSPECTIVE

Ingle and Kokate[4] showed that the impurity dipoles in $KNbO_3$ have structural origin. The $KNbO_3$ structure is formed by a close-packed arrangement of O^{2-} and K^+ ions with Nb^{5+} ions filling in the octahedral voids, and a dipole is formed when an impurity ion is accommodated in an interstitial site and has an oxygen vacancy on the octahedron in which it is situated. The impurity ion can accommodate itself either in the otherwise empty void, or replace a Nb^{5+} ion from its proper site. The formation of dipoles this way is not peculiar to $KNbO_3$,[20] and it has been observed in $PbTiO_3$ (Ref. 21) that has similar structure to $KNbO_3$. Indeed, Ingle and Kokate[4] found that the behavior of dipoles in $PbTiO_3$ and $KNbO_3$ is similar in the sense that they tend to relax as the temperature is lowered. The dipole is said to relax when the associated oxygen vacancy is filled by the neighboring oxygen. Since the $KNbO_3$ crystals grown by the technique of Deshmukh and Ingle[22] have the tendency to be oxygen deficient,[23] and the structure is suited for the formation of dipoles,[20] the existence of this type of dipole is only to be expected, as found experimentally by Ingle and Kokate.[4]

The behavior of the dipoles in $KNbO_3$ becomes particularly interesting as these dipoles tend to lie in the direction of the spontaneous polarization, and they can readily do so since the allowed directions for the spontaneous polarization and the impurity-dipole moment are the same in all the ferroelectric phases.[9] Correspondingly, the angle between the P_s direction and the impurity-dipole-moment direction can be 0°, 90° or 180° in the tetragonal phase, and 0°, 60°, 90°, and 180° in the orthorhombic phase. If the angle is anything other than 0°, the electrostatic energy of the dipole is increased. Indeed, the dipole can reduce its energy by nucleation of a suitable microdomain around it so that its dipole moment becomes parallel to the P_s direction in the region surrounding it.[2,4,9] Of course, the nucleation requires the support of

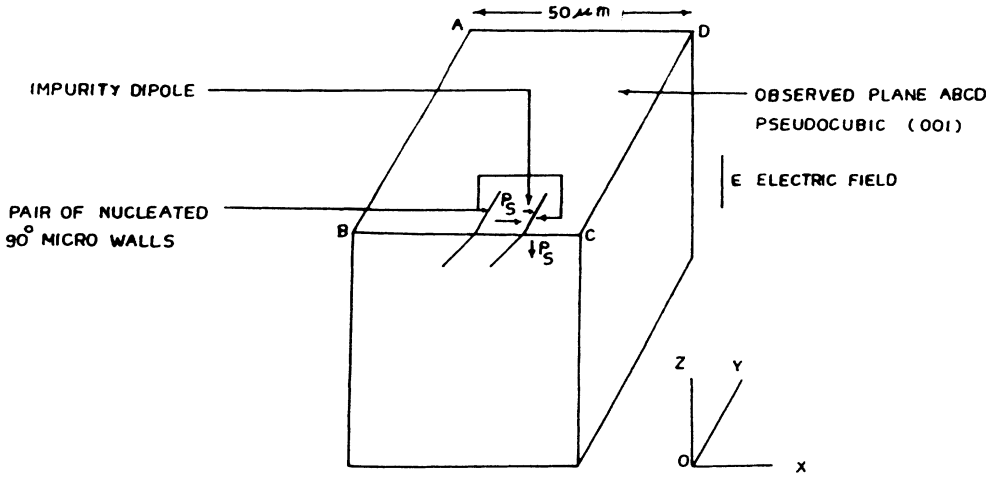

FIG. 1. A sketch showing the nucleation of a microdomain by an impurity dipole under the influence of the dc field E in the tetragonal phase of the crystal just below the Curie temperature.

the suitably applied external dc electric field. Since the magnitude of the dc field required is small, of the order of 10^4 V m^{-1}, and such fields already exist in crystals near the Curie temperature, the impurity dipoles participate in microdomain nucleation immensely, and play a stellar role in domain formation. This process of domain formation is all the more spectacular due to the cooperative ordering of the impurity dipoles near the Curie temperature. Figure 1 shows the microdomain nucleation by an individual dipole,[2] and Fig. 2, the formation of a large domain due to the cooperative ordering of the dipoles.[9] Such ordering arises form the strong, large-distance interaction among the dipoles.[7] We find that the dipoles arrange themselves in rows (Fig. 2) with the result that the microdomains they nucleate are also arranged in rows. Since the edge length of the microdomain walls is of the same order as the mutual separation of the impurity dipoles in the structure,[7] the microdomains can join each other edge to edge producing a large domain as shown in Fig. 2.

It is further found that the orthorhombic domain structures are very simply related to these tetragonal structures. For example, the orthorhombic domain structure that one would obtain from the domain structure shown in Fig. 2, is as shown in Fig. 3. It may be noted that, in this scheme of things, domain walls retain their positions at the transition, and the polar axes rotate suitably as suggested by Jona and Shirane.[24] Correspondingly, 90° tetragonal domains give rise to 60° orthorhombic domains, and 180° tetragonal domains, 90° orthorhombic domains.

III. THEORETICAL MODEL OF SWITCHING

In this model, it is assumed that the nucleation of microdomains by the impurity dipoles, and their evaporation when the field gets reversed, plays an all important part, and the part played by growth of the domains is negligible. Let the maximum possible nucleation sites be N_∞ in the volume V of the sample. Let the nucleation

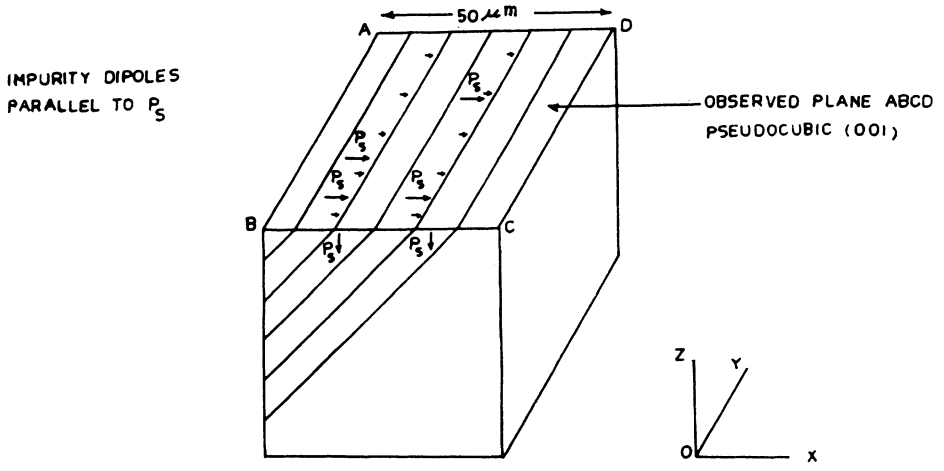

FIG. 2. A sketch explaining the formation of a large domain by joining several microdomains end to end.

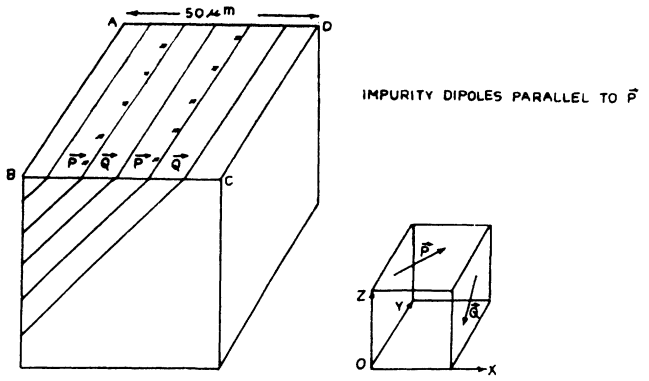

FIG. 3. A sketch showing the orthorhombic domain structure derived from the tetragonal domain structure shown in Fig. 2.

take place under the influence of the field E, at a given time t, and the number of microdomains nucleated by N. At any instant the rate of nucleation must be proportional to the sites available for nucleation. Hence, we have

$$\frac{dN}{dt} \propto (N_\infty - N) \ . \tag{3.1}$$

The relation shown in (3.1) applies generally to defects which can induce nucleation of microdomains, and only the impurity dipoles have been found to play this role[4] in $KNbO_3$. An equation can be set up from (3.1) by employing a constant that has dimensions of time. We write

$$dN = \frac{1}{\tau}(N_\infty - N)dt \ , \tag{3.2}$$

where τ is a constant with dimensions of time. Since the nucleation process depends upon the activation energy of the nucleation, which itself depends upon the field E, and temperature T as shown by Ingle *et al.*,[2] we have that τ is field and temperature dependent. Equation (3.2) readily gives

$$\int_0^N \frac{dN}{(N_\infty - N)} = \frac{1}{\tau}\int_{t_0}^{t} dt \ , \tag{3.3}$$

when t_0 is the incubation time which must elapse before the nucleation process begins. We have

$$-\ln\frac{(N_\infty - N)}{N_\infty} = \frac{t - t_0}{\tau} \tag{3.4}$$

and

$$N = N_\infty(1 - e^{-(t-t_0)/\tau}) \ . \tag{3.5}$$

Equation (3.4) gives that, if we plot $\ln(N_\infty - N)$ versus t, we should get a straight line with slope $-1/\tau$, and the intercept of the line on $\ln(N_\infty - N)$ axis equal to $(\ln N_\infty + t_0/\tau)$. Hence, both τ and t_0 can be calculated knowing the value of N_∞, which is also known as the density of the impurity dipoles is known. Alternatively, we can use the approximate relation

$$\ln\left[1 - \frac{N}{N_\infty}\right] = -\frac{N}{N_\infty} \ , \tag{3.6}$$

since N is quite small as compared to N_∞, at least in the beginning of the nucleation process. Thus, we get from Eq. (3.4),

$$N = \frac{N_\infty(t - t_0)}{\tau} \ . \tag{3.7}$$

Plotting N versus t readily gives t_0. Calculations of this type (Sec. IV) give that, for the fields used in tracing the loop, the incubation times are quite small, i.e., of the order of the periodic times of the frequencies used. Thus, the hysteresis loops can reflect the effect of this nucleation process.

When the hysteresis loop is being traced, the value of E is changing continuously at the rate depending on the frequency of tracing. Also, the polarization change is both due to the nucleation and evaporation process. At any field E and time t, as microdomains are being nucleated, the existing microdomains nucleated under the opposite field are being removed from the structure; this process is called "evaporation." Recently, Ingle and Moon[6] studied the kinetics of this process and found that a microdomain nucleated at field E requires a reverse field $\frac{3}{2}E$ for its evaporation. Considering the combined effect of nucleation and evaporation, we can write

$$\frac{dN}{dt} = A(N_\infty - N) - BN \ , \tag{3.8}$$

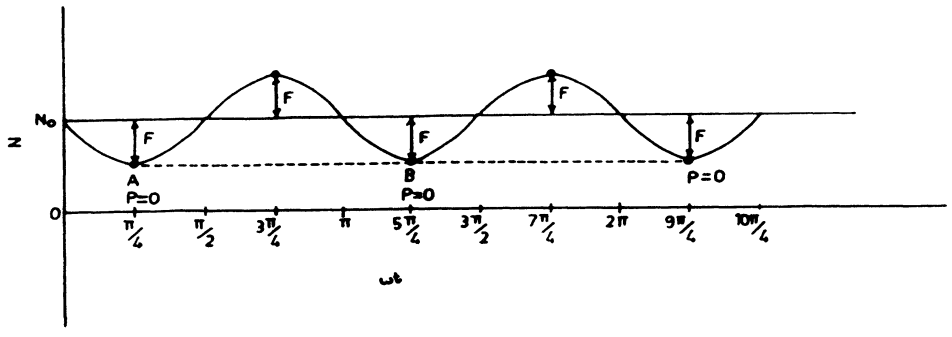

FIG. 4. A theoretical sketch showing the relation of N with phase angle (ωt) over the cycle.

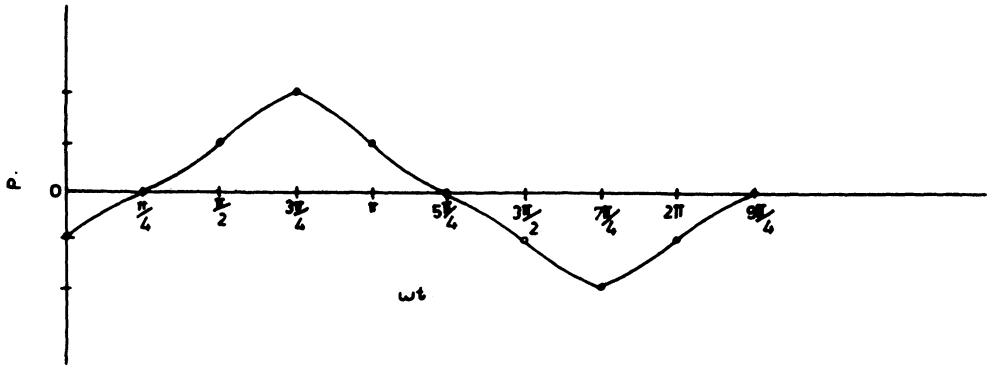

FIG. 5. A graph showing the variation of P with the phase angle over the cycle.

where A and B are constants having dimensions of time as mentioned before. The factor $(-BN)$ accounts for the evaporation process adequately as the rate of evaporation at any instant must be proportional to N, the number of microdomains existing at that instant. We have

$$\frac{dN}{dt} = AN_\infty - CN \ , \tag{3.9}$$

where

$$C = A + B \ . \tag{3.10}$$

We write

$$\frac{dN}{dt} = \frac{dN}{dE}\frac{dE}{dt} \ , \tag{3.11}$$

where

$$E = E_0 \sin(\omega t) \tag{3.12}$$

and ω is the angular frequency of tracing the ac field. Putting dN/dE proportional to E, and

$$\frac{dN}{dE} = A'E \ , \tag{3.13}$$

where A' is a constant, we get

$$\frac{dN}{dt} = \frac{A'wE_0^2}{2}\sin(2\omega t) \ . \tag{3.14}$$

Hence,

$$N = \frac{A}{C}N_\infty - \frac{A'wE_0^2}{2C}\sin(2\omega t) \tag{3.15}$$

or

$$N = N_0 - F\sin(2\omega t) \tag{3.16}$$

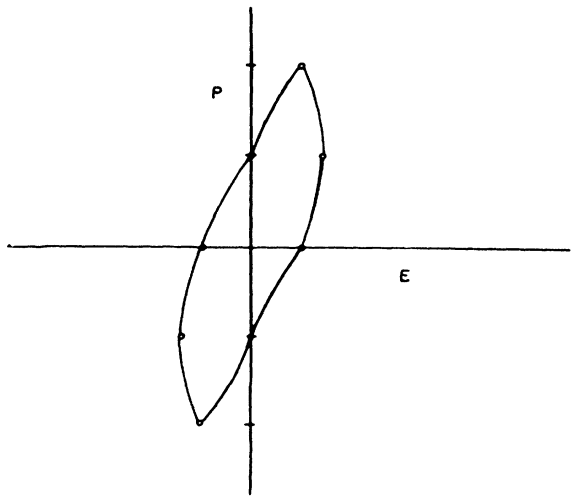

FIG. 6. P-E relationship showing the hysteresis curve obtained from the theoretical model.

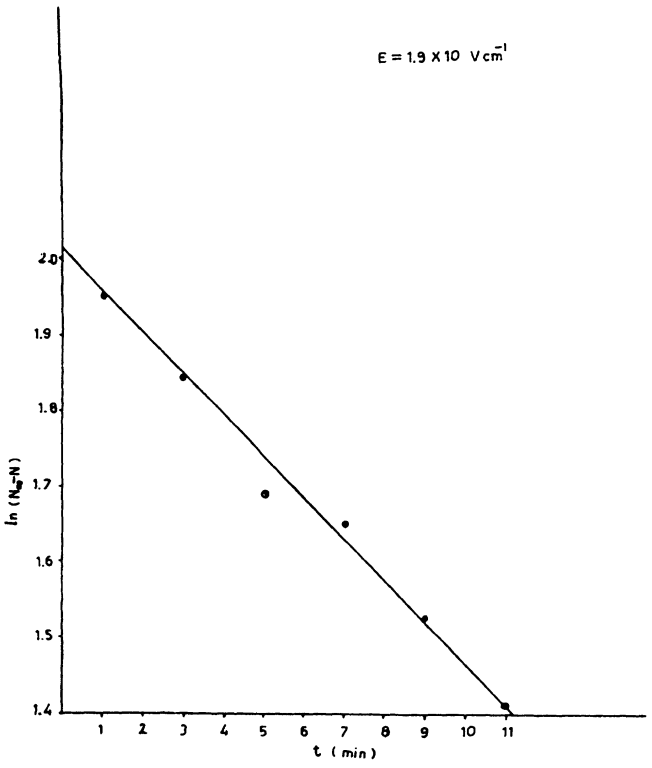

FIG. 7. A graph showing the relation between N and t under the influence of the externally applied dc field 1.9×10^3 V cm^{-1}.

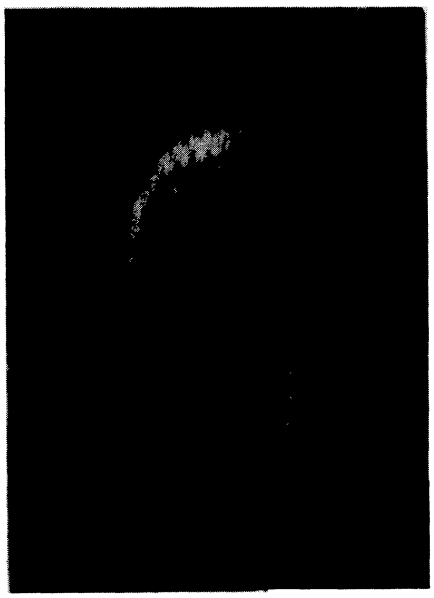

FIG. 8. A hysteresis loop observed at 1 Hz. Scale: E axis (1 div. = 500 V cm^{-1}), P axis (1 div. = 3 μC).

with

$$N_0=\frac{A}{C}N_\infty \tag{3.17}$$

and

$$F=\frac{A'wE_0^2}{2C}\ . \tag{3.18}$$

We can now plot N as a function of time using Eq. (3.16) during the hysteresis cycle. A schematic sketch of this is shown in Fig. 4. Taking (N_0-F) to correspond to $P=0$, and noting that N must correspond to opposite polarization after every half-cycle of the applied ac voltage, the changes of polarization over the cycle should be as shown in Fig. 5. When these changes are shown on the P-E graph, we get the variation depicted by Fig. 6. We find here that, indeed, a hysteresis loop is traced.

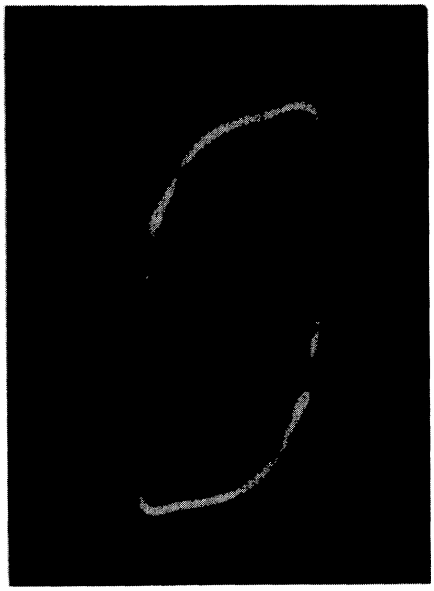

FIG. 9. The hysteresis loop of Fig. 8 traced at 6.7 Hz. Scale: E axis (1 div. = 500 V cm^{-1}), P axis (1 div. = 3 μC).

IV. EXPERIMENTAL VERIFICATION

Single crystals of $KNb0_3$ were grown by the technique of Deshmukh and Ingle.[22] Since the crystals are grown in a platinum crucible, the main impurity is that of platinum ions that get incorporated in the structure during growth. The impurity dipoles have structural origin, and therefore the chemical nature of the impurity is not of

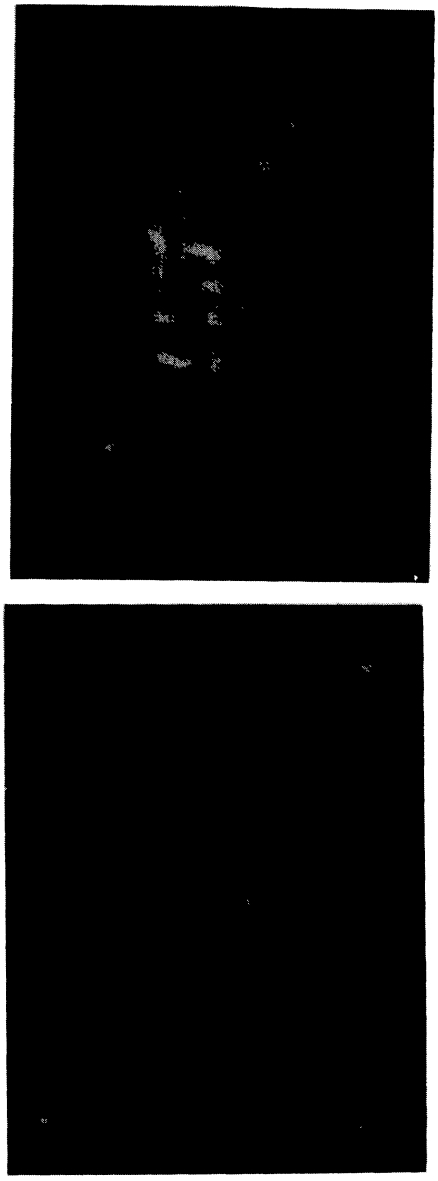

FIG. 10. A hysteresis loop showing sudden and large changes of polarization on the loop. Scale: E axis (1 div. = 500 V cm^{-1}), P axis (1 div. = 3 μC). (b) A hysteresis loop shown by the $KNbO_3$ single crystal not containing cooperatively ordered dipoles. Scale: E axis (1 div. = 500 V cm^{-1}), P axis (1 div. = 3 μC).

any consequence, as is generally true of the impurity dipoles formed by this mechanism.[20] The impurity content in the crystals used is of the order of 10^{16} m^{-3}.

The hysteresis loops were observed with the use of the standard Sawyer and Tower circuit, and no particular problems are faced because the resistivity of the crystals is high. Adjustable compressive forces could be applied to the major faces of the crystal by means of a light spring.

To verify the linear relation between N and t, the crystal was applied to a dc electric field for varying durations of time, and the number of microdomains nucleated were counted. In a particular case a field 1.9×10^3 V cm^{-1} was used, and Fig. 7 shows a graph of $\ln(N_\infty - N)$ versus t. For the small area considered, N_∞ was ~ 75, and the graph shows that t_0 is quite small, of the order of 0.1 sec though the precise determination is not possible due to the error involved in the measurement of N. However, the response of the domains can be expected to be shown in the hysteresis loops. To cover the wide spectrum of the values of t_0, the loops were observed over the frequency range 10^{-1}–10^6 Hz. The low-frequency loops show several sudden changes of polarization as, for example, marked by arrows in Fig. 8, that have been obtained at the tracing frequency 1 Hz. Since the tracing frequency was gradually changed from 1 to 6.7 Hz, (Fig. 9), it was observed that the number of sudden changes of polarization went on decreasing, and the polarization change at a given place also diminished continuously. On the model developed in the previous section, one can as-

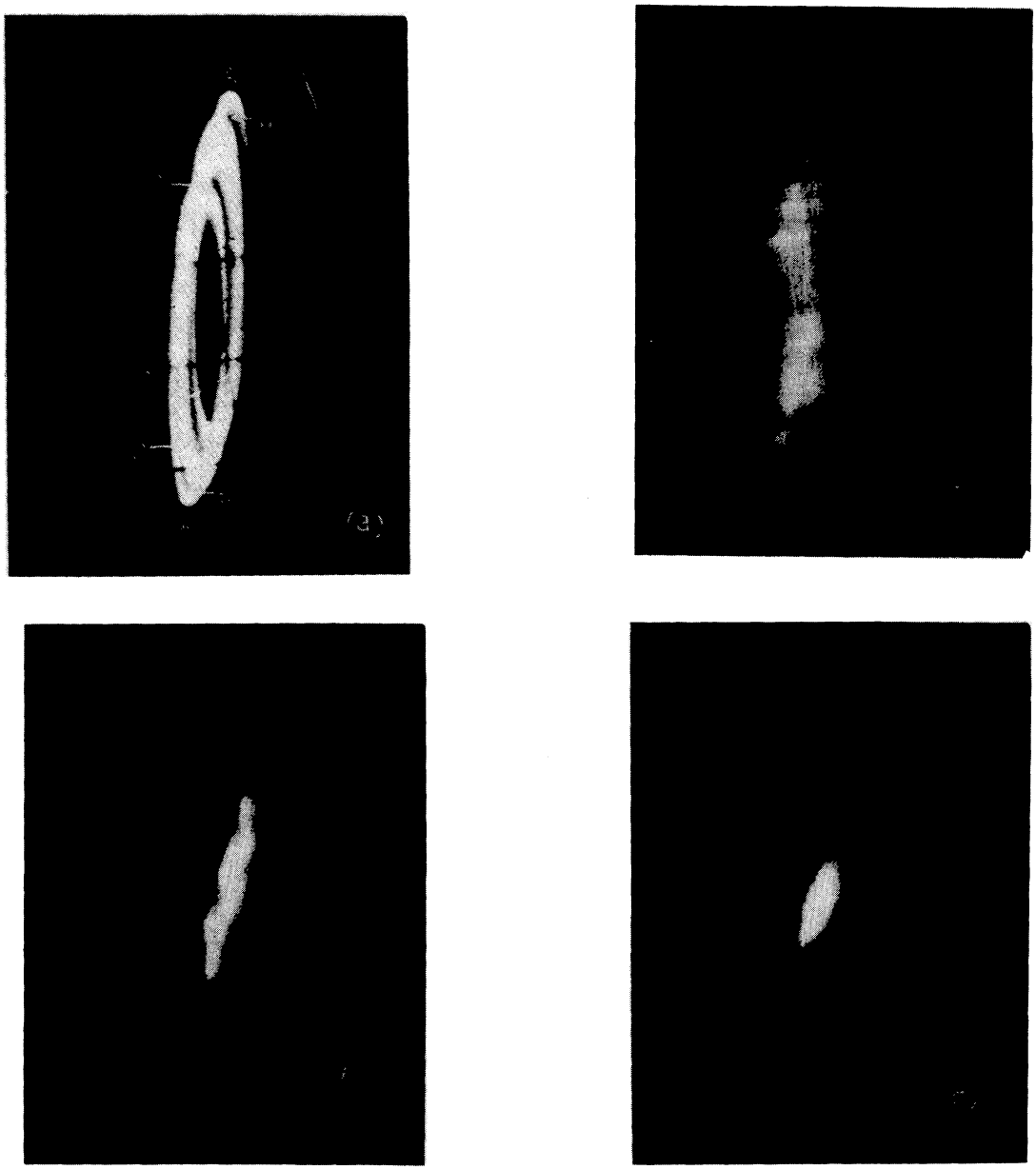

FIG. 11 The hysteresis loops traced at various tracing frequencies (a) 100, (b) 120, (c) 160, and (d) 250 KHz.

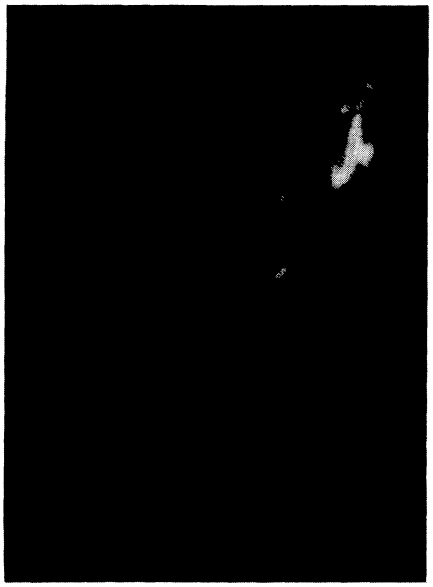

FIG. 12. A hysteresis loop traced at 100 KHz. Note the localized hysteresis loops marked *L*.

sociate a sudden change of polarization on the hysteresis loop as observed in Fig. 8 with a domain or group of domains nucleating or evaporating at that instant. As shown in Fig. 2, several microdomains can form a large domain due to cooperative ordering of the dipoles, and this large domain can respond more or less as a single unit. On this basis, the hysteresis loops, as in Fig. 10(a) (traced at 50 Hz), can be readily understood as conveying the existence of large domains in the crystal (corresponding to large changes of polarization as at *A*, *B*, etc.). For comparison, the hysteresis loop for crystals not containing cooperatively ordered dipoles is shown in Fig. 10(b). It is of the type normally obtained in ferroelectrics.

Of particular interest is the fact that the change of polarization corresponding to a particular domain in the crystal is not shown as the tracing frequency is changed. This means that the domain has a characteristic response time such that, only at the tracing frequency corresponding to this response time, the domain can show itself. Clearly, the different domains shall have different response times, and shall show their presence on the hysteresis loop at different frequencies. Thus, the observation of hysteresis loops at varying frequencies offers here a ready means of identifying different domains in the crystal. It is observed that most of the domains have their response times such that they are shown at tracing frequencies near 1 Hz.

It is to be expected that the response time is related to the incubation time that itself depends on several factors like the manner of cooperative ordering existing at the site of the domain, the type of the domain to be nucleated, i.e., 60°, 90°, or 180°, the size of the domain determined by the number of impurity dipoles participating in the nucleation process, and the other local conditions of strain, etc. At high frequencies only a few domains respond, and the way they show themselves is totally different from the way the domains show themselves at low frequencies. We find that, at high frequencies, the domains produce separate hysteresis loops as the normalized incubation times, viz., t_0/T, where T is the periodic time of the tracing ac voltage, are quite separated from each other. Before a particular domain starts showing itself, the other has already finished its hysteresis loop due to the small periodic time of the ac voltage used. In the process, both the loops are shown on the screen. Also,

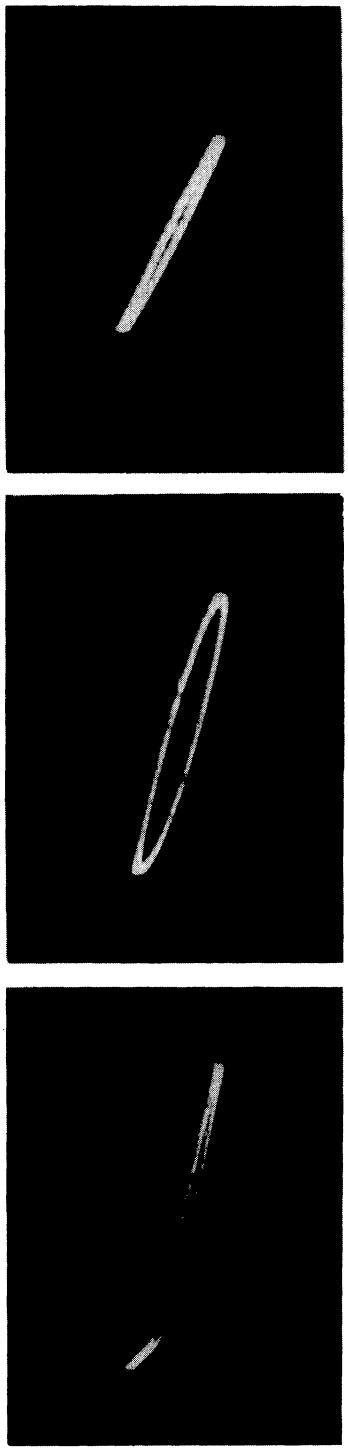

FIG. 13. The hysteresis loops traced at various tracing frequencies (a) 10, (b) 50, and (c) 70 KHz.

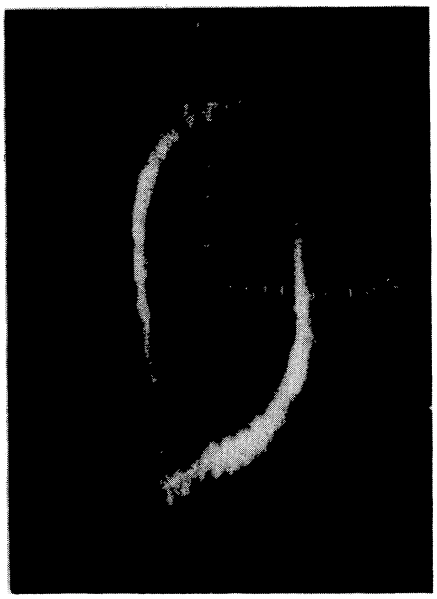

FIG. 14. A hysteresis loop traced at 1 Hz. Scale: E axis (1 div. $=500$ V cm^{-1}), P axis (1 div. $=3$ μC).

there occurs considerable change in the shape of the hysteresis loop as the tracing frequency is changed. The photographs in Figs. 11 (a)–11 (d) show, respectively, the loops at 100, 120, 160, and 250 kHz. In Fig. 11 (a), one can see three distinct hysteresis loops, AA, BB and CC, corresponding to three domains in the crystal. The other domains in the crystal are not responding at this tracing frequency and, hence, are not represented in the photograph. As the frequency is increased, these three domains have response times not quite matching with the tracing frequency, while some other domains start showing themselves. Thus, there is considerable difference between the picture seen in Fig. 11(a) and Fig. 11(b). The responses in Figs. 11(c) and 11(d) can be noted for comparison. Not only have the different loops merged into each other here, but the shape of the loop has also diminished.

Figure 12 shows an altogether different type of situation. We find that two localized hysteresis loops marked L on the photograph are seen. These are not due to domains, but small crystallites mismatched from the rest of the crystal. The crystallite is already placed in polarization and electric field about which it shows variation, and, hence, a localized hysteresis loop.

The observed coercive fields are found to depend on the frequency of measurement and should not be con-

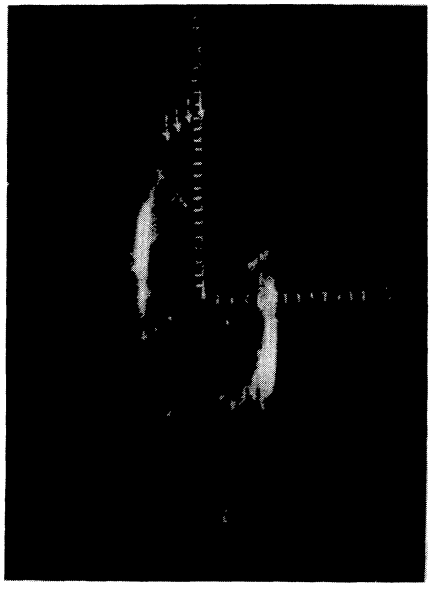

FIG. 15. The hysteresis loop of Fig. 14 when the dc bias field 6×10^4 V m^{-1} was applied to the crystal. Scale: E axis (1 div. $=500$ V cm^{-1}), P axis (1 div. $=3$ μC).

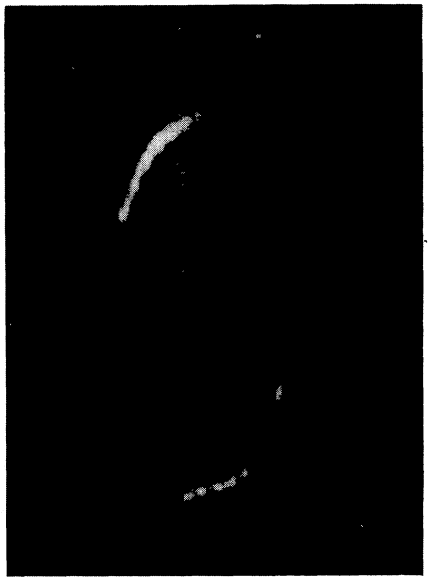

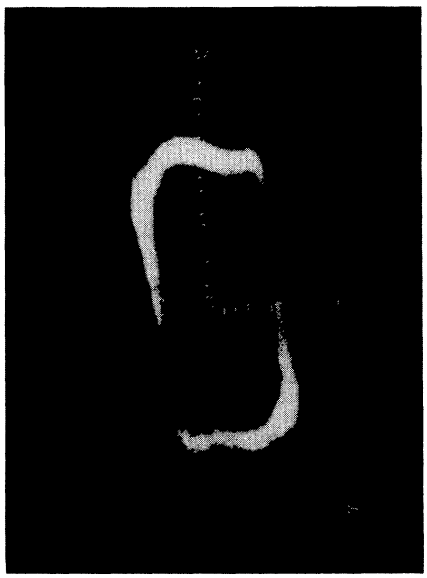

FIG. 16. (a) A hysteresis loop traced at 1 Hz. Scale: E axis (1 div. $=500$ V cm^{-1}), P axis (1 div. $=3$ μC). (b) The hysteresis loop of (a) when slight compressive mechanical forces were applied to the crystal. Scale: E axis (1 div. $=500$ V cm^{-1}), P axis (1 div. $=3$ μC).

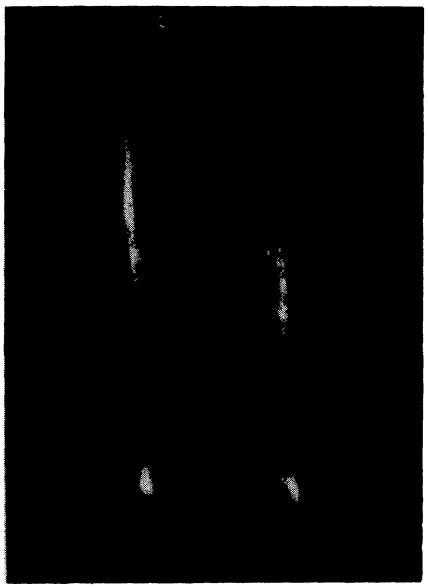

FIG. 17. A hysteresis loop traced at 400 °C, the tracing frequency being 1 Hz. Scale: E axis (1 div. $=500$ V cm^{-1}), P axis (1 div. $=3$ μC).

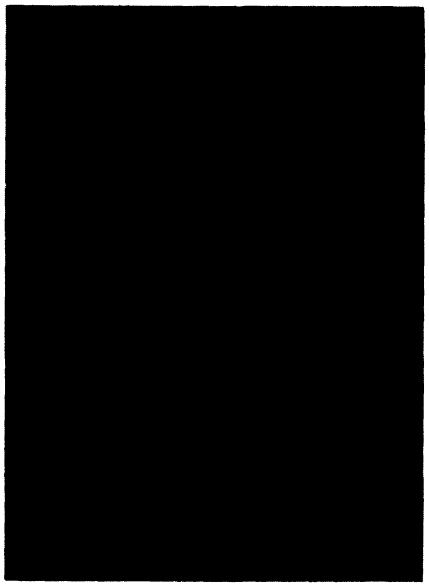

FIG. 18. A switching transient observed in the $KNbO_3$ single crystal containing cooperatively ordered impurity dipoles.

fused with the coercive fields normally obtained from such measurements. For example, Figs. 13(a)–13(c) show hysteresis loops at tracing frequencies 10, 50, and 70 kHz, respectively. It can be readily seen that the coercive field does not fall regularly with the increase in frequency, as is normally the case. Rather, we find that the coercive field has increased here in Fig. 13(b) but decreased in Fig. 13(c), though the frequency is increased in both cases.

That the impurity-dipole-related domains respond in a different way from the rest of the domains can be readily seen by providing an external clamping effect either by providing dc bias fields, or by applying compressive forces to the major faces of the crystal by means of a light spring. It is found that, while the rest of the domains get clamped, the impurity-dipole-related domains do not get clamped, and therefore one can observe only the impurity-dipole-related part of the hysteresis loop, and also more clearly, since the effect of the rest of the domains is not superposed on it. For example, Fig. 14 shows a hysteresis loop at 1 Hz without any bias field. The same crystal shows the loop as in Fig. 15 when a bias field 6×10^4 V m^{-1} was applied to the crystal. The large changes of polarization that are seen in Fig. 15 (marked by arrows) are not seen in Fig. 14, clearly due to the superposition effect.

The photographs shown in Figs. 16(a) and 16(b) are still more interesting. No clamping is used for Fig. 16(a), while Fig. 16(b) has been obtained with mechanical clamping keeping the tracing frequency 1 Hz the same. Interestingly enough, the loop in Fig. 16(b) is a square one that is typically taken as a single domain response. In the present case, however, the interpretation is that the crystal contains a large impurity-related domain that has a response time matching with the tracing frequency 50 Hz, and other domains that have response time far removed from this time. Also, since other nonimpurity-related domains are clamped, their effect is not shown as it is shown in Fig. 16(a), enabling the effect of the impurity-related domain to be seen with such clarity.

Since the nucleation times should reduce as the temperature is increased, temperature-dependent changes in hysteresis loop shapes must be expected, and have indeed been found. Also, at temperatures near the Curie temperature, the responses of the domains are very prominent, and the changes of polarization large. A typical photograph taken at 400 °C using a tracing frequency 1 Hz is shown in Fig. 17. No clamping has been used here, and the response of the impurity-related domains is seen to be spectacularly superposed on the response of the rest of the domains.

The switching transients obtained by using square-wave pulses also clearly reflect the sudden large changes of polarization that occur. Figure 18 shows a typical switching transient wherein the sudden rise in current, i.e., dP/dt, is clearly seen.

Thus, the theoretical model developed in Sec. III is found to be satisfactorily verified under variety of conditions of measurement. These experiments also confirm the ideas used in the model, viz., the ideas of microdomains nucleation,[2] cooperative ordering of the impurity dipoles,[9] and the role of the impurity dipoles in domain formation.[4]

V. CONCLUSION

It is thus found that the mode of switching in $KNbO_3$ single crystals containing cooperatively ordered impurity dipoles is essentially different from the one normally observed in this crystal. The switching under these conditions follows the theoretical model developed on the assumption that nucleation and evaporation of microdomains play a major role in polarization reversal rather than the growth of domains. The frequency dependence of the distorted hysteresis loops and the associated pecu-

liarities of the various types can be satisfactorily explained on the basis of the ideas used in the development of the model. The nature of the switching transients obtained using square-wave pulses is also in agreement with the model. Incidentally, the model of microdomain nucleation suggested by Ingle, *et al.*,[2] and the role of the impurity dipoles in domain formation through cooperative ordering are also confirmed. For the first time, a direct correlation has been obtained between the hysteresis loop shapes and the domain structures.

ACKNOWLEDGMENT

The authors are thankful to Professor H. Klapper, Mineralogisches Institut, University of Bonn, D-5300 Bonn, for fruitful discussions.

[1]W. Merz, Phys. Rev. **95**, 690 (1954).
[2]S. G. Ingle, H. S. Dutta, and A. P. David, J. Appl. Phys. **59**, 4640 (1988).
[3]S. G. Ingle, H. S. Dutta, and A. P. David, J. Phys. D **21**, 1239 (1988).
[4]S. G. Ingle and M. V. Kokate, Philos. Mag. A **61**, 543 (1990).
[5]S. G. Ingle and K. S. Moon, Ind. J. Pure Appl. Phys. **28**, 574 (1990).
[6]S. G. Ingle and K. S. Moon, Ferroelectrics **119**, 107 (1991).
[7]S. G. Ingle and J. G. Dupare, Pramana **36**, 167 (1991).
[8]S. G. Ingle and J. G. Dupare, Ind. J. Pure Appl. Phys. **29**, 427 (1991).
[9]S. G. Ingle, K. S. Moon, and R. N. Kakde, Bull. Mater. Sci. (to be published).
[10]J. Fousek and B. Berezina, J. Phys. Soc. Jpn. **19**, 830 (1964).
[11]A. Jaskiewicz, Acta Phys. Polon. **27**, 637 (1965).
[12]H. G. Unruh, Phys. Kondens. Mater. **4**, 275 (1965).
[13]A. Jaskiewicz and J. Bednarczyle, Acta Phys. Polon. **28**, 291 (1965).
[14]J. Silver, E. A. D. White, and V. M. Wood, J. Mater. Sci. **10**, 2010 (1975).
[15]V. A. Maleshina, Kristallografiya **16**, 557 (1971).
[16]A. Yu. Kudzin, L. G. Guskina, and I. S. Petrushkevich, Fiz. Tverd. Tela **6**, 92 (1964) [Sov. Phys. Solid State **6**, 75 (1964)].
[17]E. Maurer, B. J. Menez, C. Alemany, and J. Mendiola, An. Fis. **71**, 22 (1975).
[18]O. Boser and D. N. Beshero, in MRS Symposia Proceedings No. 82 (Materials Research Society, Pittsburgh, 1987), p. 441.
[19]O. Boser, J. Appl. Phys. **62**, 1344 (1987).
[20]J. Prakash, A. K. Nishad, and Rahul, J. Appl. Phys. Rev. **23**, 1403 (1984).
[21]G. A. Samara, Jpn. J. Appl. Phys. **24**, 24 (1985).
[22]K. G. Deshmukh and S. G. Ingle, J. Phys. D **4**, 124 (1971).
[23]S. G. Ingle and S. C. Joshi, Phys. Rev. B **34**, 4840 (1986).
[24]F. Jona and G. Shirane, *Ferroelectric Crystals* (Pergamon, New York, 1962), p. 112.

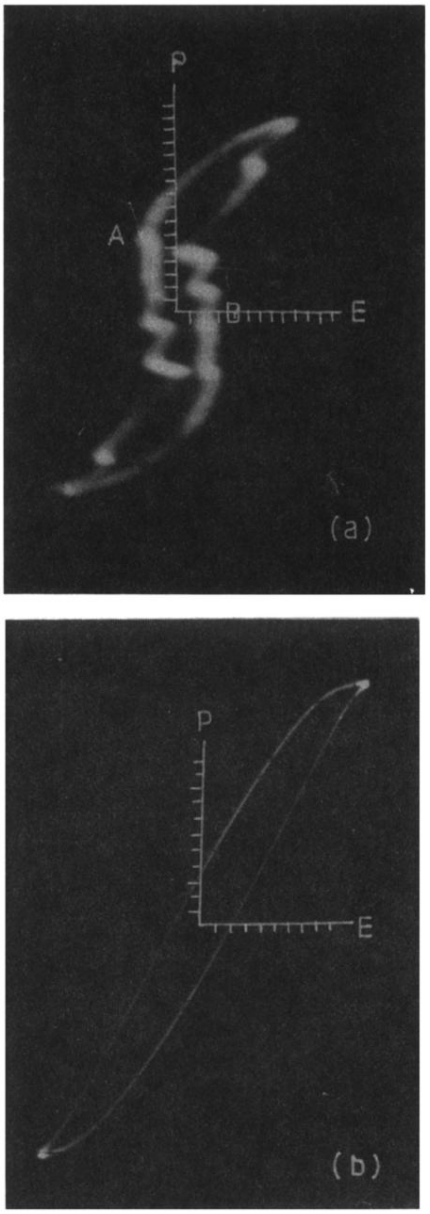

FIG. 10. A hysteresis loop showing sudden and large changes of polarization on the loop. Scale: E axis (1 div. $=500$ V cm^{-1}), P axis (1 div. $=3$ μC). (b) A hysteresis loop shown by the $KNbO_3$ single crystal not containing cooperatively ordered dipoles. Scale: E axis (1 div. $=500$ V cm^{-1}), P axis (1 div. $=3$ μC).

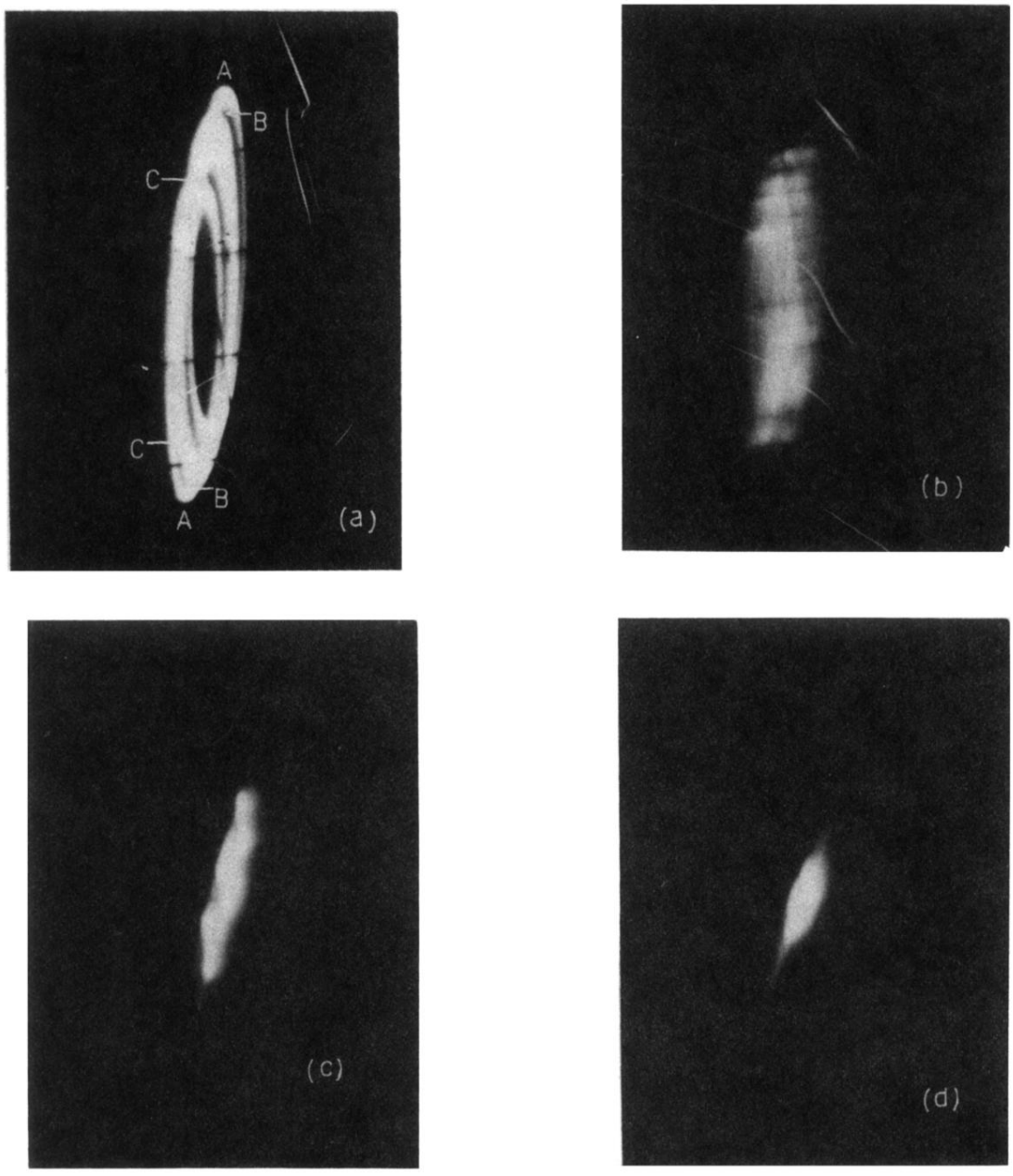

FIG. 11 The hysteresis loops traced at various tracing frequencies (a) 100, (b) 120, (c) 160, and (d) 250 KHz.

FIG. 12. A hysteresis loop traced at 100 KHz. Note the localized hysteresis loops marked *L*.

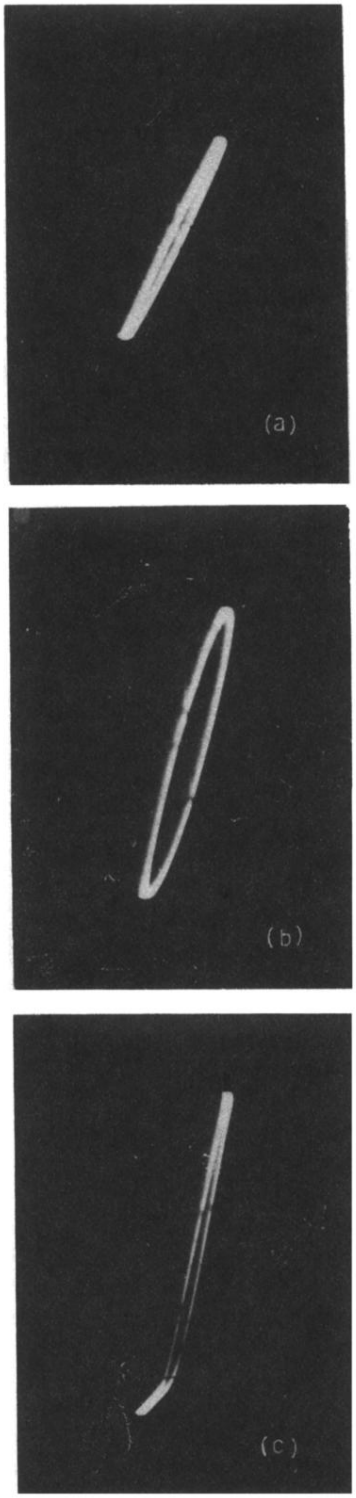

FIG. 13. The hysteresis loops traced at various tracing frequencies (a) 10, (b) 50, and (c) 70 KHz.

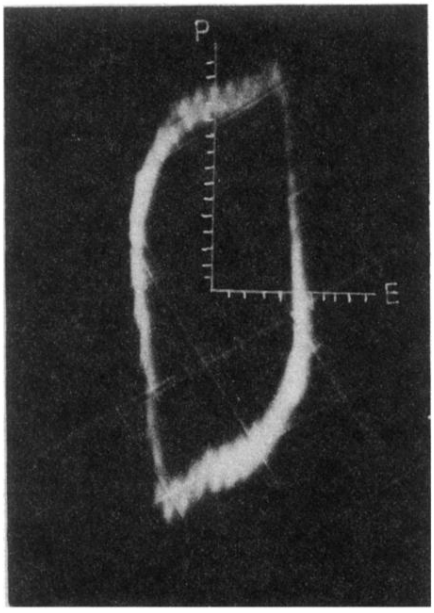

FIG. 14. A hysteresis loop traced at 1 Hz. Scale: E axis (1 div. $=500$ V cm^{-1}), P axis (1 div. $=3\,\mu$C).

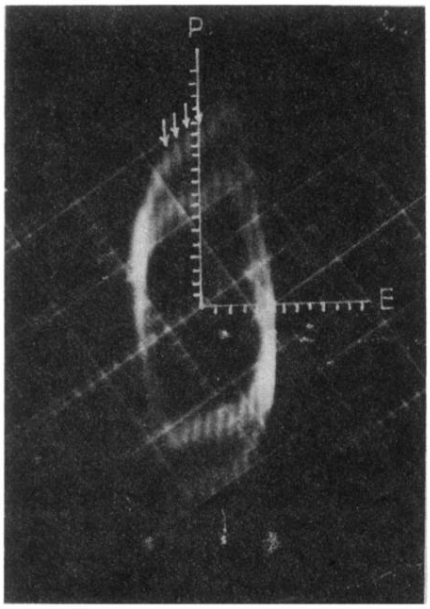

FIG. 15. The hysteresis loop of Fig. 14 when the dc bias field 6×10^4 V m^{-1} was applied to the crystal. Scale: E axis (1 div. $=500$ V cm^{-1}), P axis (1 div. $=3\,\mu$C).

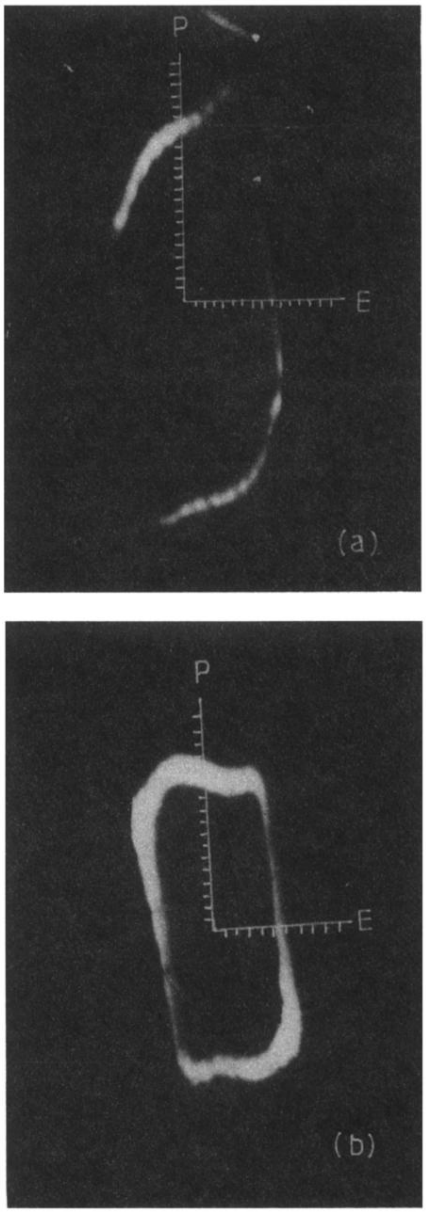

FIG. 16. (a) A hysteresis loop traced at 1 Hz. Scale: E axis (1 div. $=500$ V cm^{-1}), P axis (1 div. $=3$ μC). (b) The hysteresis loop of (a) when slight compressive mechanical forces were applied to the crystal. Scale: E axis (1 div. $=500$ V cm^{-1}), P axis (1 div. $=3$ μC).

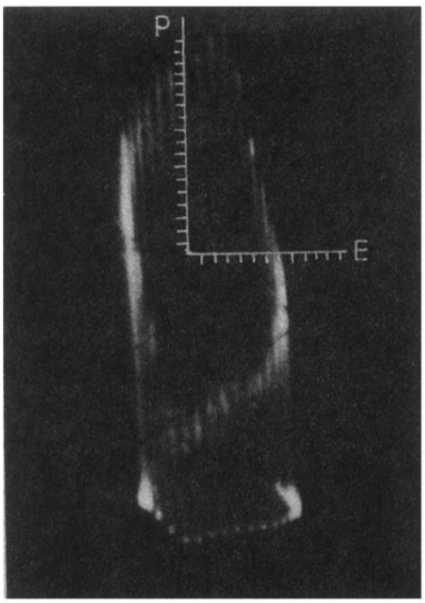

FIG. 17. A hysteresis loop traced at 400 °C, the tracing frequency being 1 Hz. Scale: E axis (1 div. $=500$ V cm^{-1}), P axis (1 div. $=3\ \mu$C).

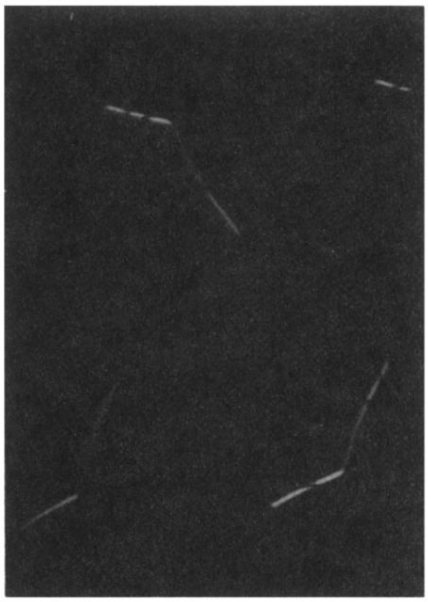

FIG. 18. A switching transient observed in the $KNbO_3$ single crystal containing cooperatively ordered impurity dipoles.

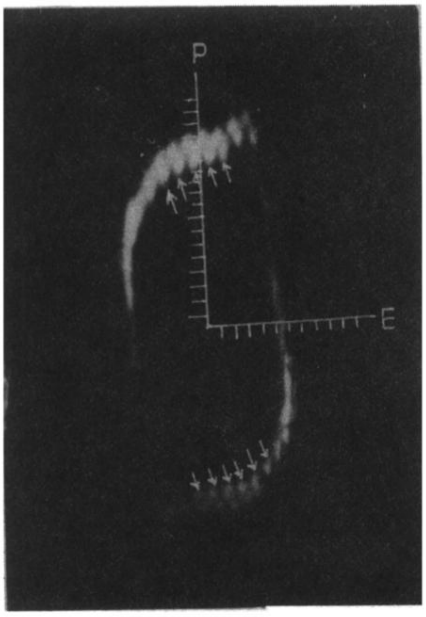

FIG. 8. A hysteresis loop observed at 1 Hz. Scale: E axis (1 div. = 500 V cm^{-1}), P axis (1 div. = 3 μC).

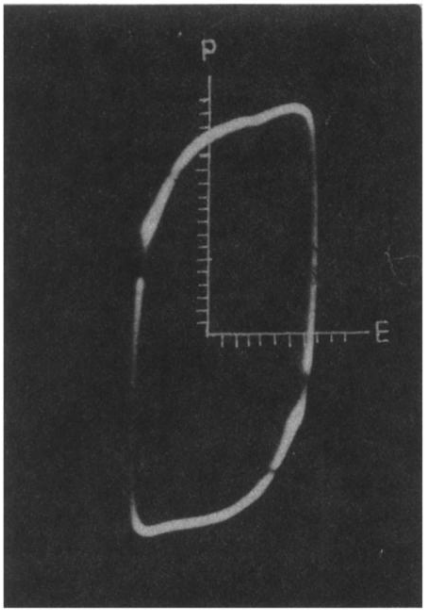

FIG. 9. The hysteresis loop of Fig. 8 traced at 6.7 Hz. Scale: E axis (1 div. = 500 V cm^{-1}), P axis (1 div. = 3 μC).